Global Journal of Engineering and Technology Advances
eISSN: 2582-5003
Cross Ref DOI: 10.30574/gjeta
Journal homepage: https://gjeta.com/

(RESEARCH ARTICLE)

Check for updates

Classification and comparison of glaucoma detection methods in retinal fundus images using SVM and U-Net2

Aaron García-Campos, Javier Rodríguez-Herrejón *, Enrique Reyes-Archundia, Arturo Mendez-Patiño and Jose A. Gutiérrez-Gnecchi

Division for Postgraduate Studies, Technological Institute of Morelia, Morelia, Mexico.

Global Journal of Engineering and Technology Advances, 2025, 22(03), 155-164

Publication history: Received on 11 February 2025; revised on 20 March 2025; accepted on 22 March 2025

Article DOI: https://doi.org/10.30574/gjeta.2025.22.3.0070

Abstract

In medical image processing, early detection of eye diseases like glaucoma is crucial to prevent blindness. This study evaluates two deep learning models—Support Vector Machine and U-Net—for classifying retinal fundus images to improve glaucoma detection. Using 316 images from "The Brazil Glaucoma Database," the study applied various preprocessing techniques such as resizing, grayscale conversion, and edge enhancement. Optical disc and cup segmentation was achieved with Hough transform and circular masking. The SVM model outperformed U-Net, achieving 95% accuracy compared to U-Net's 88%. SVM showed better precision, recall, and F1-scores, making it more reliable for distinguishing between normal and glaucoma images. While U-Net had strong recall for glaucoma detection, its lower precision and accuracy indicate room for improvement. Future work should focus on refining U-Net to enhance its precision and overall performance.

Keywords: Retinal Fundus; Glaucoma; Digital Image Processing; Svm; U-Net

1 Introduction

Image processing within the medical field, particularly through the application of Deep Learning techniques, has seen significant growth and is increasingly dominating the analysis of medical data and images. This includes the diagnosis of various conditions such as glaucoma (including its different types), diabetic retinopathy, and age-related macular degeneration, among others [1].

The algorithms employed in this type of processing rely on feature extraction techniques, ranging from low-level methods to advanced Deep Learning techniques. These approaches primarily utilize retinal fundus images and optical coherence tomography (OCT) [2]. Additionally, the analysis of other characteristics based on images obtained from the eye is feasible.

There are several other eye diseases, such as tumors [3], diabetic macular edema, and cataracts, which can also be detected using these techniques. These diseases share the common characteristic of being difficult to detect early, yet early detection is crucial for preventing permanent blindness [4].

Prototypes have been developed for the detection of glaucoma using high-resolution smartphone cameras [5]. Additionally, some systems employ smartphones connected to a Welch Allyn panoptic direct ophthalmoscope [6]. There has also been a comparison of various digital ophthalmoscopes available on the market [7].

* Corresponding author: Javier A. Rodríguez-Herrejón

For training detection systems, various datasets are utilized, some of which are publicly accessible [4]. Additionally, custom datasets can be created using high-resolution commercial cameras [6].

Studies on the detection of ocular diseases through image processing depend largely on the specific diseases being investigated. However, within this variety, certain characteristics can be highlighted, which are obtained through the preprocessing and processing of ocular images acquired through various methods.

Some of the most commonly used ocular images for disease detection are fundus imaging [8-13], and OCT [1,14]. Although these are not the only types, they are the most frequently utilized for detecting eye diseases such as glaucoma, due to the significant information contained in the retinal vascular structures.

Additionally, other imaging modalities that can be used include PET-CT, ocular ultrasound, angiography [3], 3D OCT [15], scanning laser ophthalmoscope (SLO), and fluorescein angiography (FA) [16].

Once these images are available, image processing is conducted to extract and detect features such as the measurements of the Optical Cup (OC) and the Optical Disc (OD) in the retina [11,12,17]. This is achieved through classification and segmentation algorithms based on machine learning, which facilitate the detection of glaucoma by analyzing the relationship between these two measurements. Furthermore, other measures for glaucoma detection include the inferior, superior, nasal, and temporal quadrants, collectively known as the ISNT quadrants [11].

Certain diseases, such as ocular tumors [3], cataracts, myopia, diabetic retinopathy, age-related macular degeneration, and glaucoma [18, 19], can be effectively treated if detected at an early stage. For early diagnosis, some necessary measurements can be obtained using deep learning approaches, such as retinal vessel segmentation and retinal layer and fluid segmentation methods [20]. Generally, it is feasible to develop models based on a combination of classical image processing algorithms and artificial intelligence that can detect the onset of glaucoma or other diseases based on specific parameters of the retinal fundus [13].

Table 1 below presents accuracy results from various studies related to the detection of glaucoma.

Table 1 Comparison of glaucoma detection accuracy

Ref	Technique or method	Accuracy
[3]	This work proposes a deep convolutional neural network (CNN) based on a modified LeNet architecture. To identify the regions of interest encompassing the eyeball and iris, a Hough circle transformation is employed.	95%
[8]	The work proposes to obtain the value of the Cup-to-Disc radius, which they consider must be equal to or greater than 0.6 to be considered glaucomatous, they perform the segmentation of the disc based on an algorithm that is based on the histogram in the "red" matrix, and through a threshold through an intelligent algorithm they perform the segmentation of the cup.	88.5%
[10]	A Le-Net architecture, validates the input image format. To identify the crucial optic disc region, the system employs a brightest spot detection algorithm. Then, a U-Net architecture, tackles optic disc and optic cup segmentation, separating the neural tissue from the surrounding excavated area. Finally, machine learning takes center stage with a Support Vector Machine (SVM), neural network, and Adaboost classifiers analyzing the segmented features to classify the image as healthy or indicative of glaucoma.	98.67%
[12]	To pinpoint the crucial optic nerve region, a pre-trained deep learning model called ResNet-50, a type of region-based convolutional neural networks (R-CNN), is employed for glaucoma fundus image localization. Once the region is localized, a gradient-color-based technique is used for cup-to-disk area segmentation, separating the optic disc from the surrounding optic cup (excavated area). This segmentation allows for calculating the cup-to-disc ratio, a vital indicator of glaucoma.	95%
[15]	The model employs a multi-pathway architecture where one pathway receives the original 3D data, while the others receive modified versions based on the attention guidance.	93.8%
[19]	The proposed model utilizes pre-trained deep learning algorithms, specifically ResNet and VGG16, to analyse medical images. These algorithms are essentially CNN trained to identify patterns in images.	92%

[21]	It proposes a CNN. To ensure the model's generalizability and prevent overfitting, a validation technique called K-Fold Cross Validation is employed. The effectiveness of the CNN is evaluated using various metrics like accuracy, recall, specificity, precision, and F1-score. Additionally, ROC curves are likely used to visualize the model's performance.	99.89%

This paper presents a comparison of a classification algorithm based on SVM against a U-Net2 algorithm to compare the efficiency of the two aforementioned classifiers. From the database (Provided by "The Brazil Glaucoma database" [22], https://globaleyeh.com/), we extracted 316 images; 158 images of patients with glaucoma and 158 images of patients without glaucoma.

Digital image pre-processing techniques are used: resizing the images, converting to gray scale, performing anti-aliasing filtering, applying normalization to the image, and highlighting edges. The segmentation and detection of the circles was carried out using the Hough transform on the image to obtain the optical disk. Subsequently by creating a circular mask that is applied to the original image using bitwise operations to isolate the region of the optic disc to obtain the segmented region of the optic cup. The SVM and U-NET classifiers were applied to compare their respective efficiency, recall and F1-score.

2 Retinal Fundus Images and Their Relationship with Glaucoma

Glaucoma is characterized by the progressive degeneration of retinal ganglion cells and their axons, leading to alterations in the optic nerve head and the retinal nerve fiber layer, ultimately resulting in vision impairment and irreversible blindness [23].

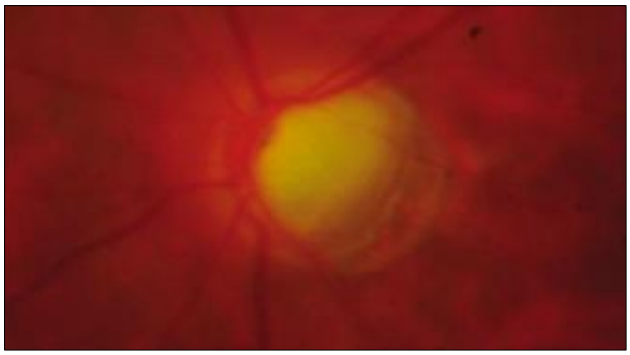

Figure 1 The picture of eye retinal fundus has glaucoma, as seen by a large cupped optic nerve and thinning tissue around it in the retinal image [23].

Given the slow progression of glaucoma and the irreversible nature of neuronal damage, early diagnosis and sensitive monitoring of disease progression are crucial for effective treatment. Structural measurements, such as retinal fundus photography, are commonly utilized in clinical evaluations for glaucoma, this type of photo is shown in Figure 1.

Retinal fundus photography is a well-established, cost-effective imaging technique used to identify features in the retinal fundus region, including the fovea, macula, OD, and OC. Glaucoma identification often involves examining the optic nerve head, where the cup-to-disc ratio (CDR) is a critical biomarker. The CDR is defined as the ratio of the vertical diameter of the optic cup to that of the optic disc. An elevated CDR value is indicative of a higher likelihood of glaucoma [23].

3 Techniques used for digital image processing

The detection of glaucoma in retinal fundus photographs involves the application of several advanced image processing techniques and computational algorithms. These methods enhance the quality of the images and facilitate the accurate identification of key anatomical features. This section elaborates on the primary techniques employed in this study: Bilateral Filtering, Gamma Correction in digital images, Hough Transform, and the HSV color space as implemented using OpenCV.

3.1 Bilateral filter

Bilateral Filtering is utilized to smooth the images while preserving edges, which is crucial for maintaining the integrity of retinal structures such as blood vessels and the optic disc. This filter reduces noise and enhances the visibility of fine details, aiding in the subsequent analysis [24].

The bilateral filter extends the concept of linear image smoothing by incorporating a photometric weight w_p alongside the spatial weight w_s. Applied to the original image E, the bilateral filter produces the resulting image F as follows:

$$F(x) = \frac{\sum_{t \in S_m} w_s(\|t\|) w_p\left(E(x) - E(x-t)\right) E(x+t)}{\sum_{t \in S_m} w_s(\|t\|) w_p\left(E(x) - E(x-t)\right)} \quad \text{.....(1)}$$

where S_m is generally a square window $[-m, m] \times [-m, m]$. The spatial weight w_s is a symmetric function that decreases with the distance $\|t\|$ from the center of S_m. Similarly, the photometric weight w_p is typically an even function that decreases with intensity [24].

3.2 Gamma correction in digital images

Gamma Correction is an image processing technique used to adjust the brightness and contrast of digital images. This method applies a nonlinear transformation to the pixel intensity values, allowing for the enhancement of image details that may not be visible with linear adjustments [25]. By modifying the gamma value, the technique can brighten dark regions and tone down overly bright areas, resulting in a more balanced and visually appealing image. Its basic form can be formulated as:

$$T(l) = l_{max} \left(\frac{l}{l_{max}}\right)^{\gamma} \quad \text{.....(2)}$$

where γ represents the gamma parameter and l denotes the pixel intensity. For simplicity, we consider an 8-bit grayscale image where l ranges from 0 to 255. The maximum pixel intensity l_{max} of the input image is typically set to 255. The intensity l of each pixel in the input image is transformed according to $T(l)$. Rather than using a fixed value, the gamma parameter can be adjusted based on statistics extracted from the input images [25].

3.3 Hough Transform

The Hough Transform is a powerful tool for finding specific shapes in images, not just straight lines and being widely used to find circles [26]. It works by creating a special map where each point represents a possible distance and angle from a central point (often the top-left corner). Imagine dropping a line perpendicular to the shape from this central point [26]. The distance between them is called ρ, and the angle this line makes is called θ. Its basic mathematical expression is:

$$\rho = x^* cos(\theta) + y^* sin(\theta) \text{.....(3)}$$

The Hough Transform takes each edge point in a black and white image and votes for the corresponding distance and angle in this map [26].

3.4 HSV color space – OpenCV

The HSV (Hue, Saturation, and Value), simulates how colors seem when illuminated, each color is represented by a radial slice of the model, with black at the bottom and white at the top representing the neutral hues along the center axis [27]. Fully saturated colors are placed around a circle at a lightness value of ½, values of 0 and 1 represent pure black and white, respectively. Maximum lightness in HSV is the same as shining a white light on a colored object. HSV fail to properly disentangle color into its three value components because of humans see color. Changning the saturation makes a noticeable difference in perceived brightness even when maintaining a constant “V” or “L” level [27].

4 Implemented classifiers

In the detection of glaucoma from retinal fundus images, the choice of classifiers plays a crucial role in achieving accurate and reliable results. This section discusses the primary classification techniques utilized in this study: SVM and U-Net Architecture.

4.1 The Support Vector Machine

The SVM is a robust and adaptable family of supervised machine learning algorithms, are widely used for regression and classification tasks. The core principle of SVM is to identify the optimal hyperplane in the feature space that separates multiple classes. In binary classification scenarios, this hyperplane maximizes the margin, which is the distance between the hyperplane and the nearest data points from each class [28].

SVM also excels in non-linear situations by employing kernel functions to map input data into higher-dimensional spaces. Commonly used kernel functions include the radial basis function (RBF), sigmoid, and polynomial kernels [28]. The margin's concept is pivotal for SVM's success, as a larger margin signifies a more robust and accurate model. SVM aims to find the hyperplane that both classifies the data correctly and maximizes this margin. SVM is particularly beneficial in cases where the dataset is small but contains complex patterns [28].

In a binary classification task with two classes labeled +1 and -1, the training dataset consists of input feature vectors (X) and corresponding class labels (Y). The equation of the linear hyperplane is represented as follows:

$$w^{Tx} + b = 0 \qquad \ldots\ldots\ldots\ldots(4)$$

The vector *w* represents the normal vector, which is perpendicular to the hyperplane, and the parameter b indicates the displacement of the hyperplane from the origin along the *w* normal vector [28]. The distance between a data point x_i and the decision boundary can be calculated using:

$$d_i = \{w^{Tx} x_i + b\}/\{\|w\|\} \quad \ldots\ldots\ldots\ldots(5)$$

where $\|w\|$ denotes the Euclidean norm of the weight vector *w*.

4.2 U-Net Architecture

The U-Net architecture, features two main pathways: a contracting path and an expanding path [29]. The contracting path functions similarly to a standard convolutional neural network, repeatedly applying a block of operations consisting of two 3x3 convolutions (without padding), followed by a ReLU activation function (which allows only positive values), and a max pooling operation that halves the image size [29]. This downsampling process aids in identifying larger features, with the number of channels doubling after each downsampling step to capture more complex information.

The expanding path works to restore the original image size while retaining precise details. Each step in this path involves upsampling the reduced feature map, followed by a specialized convolution that decreases the number of channels [29].

Regular convolutions remove some edge pixels, so the network uses cropped feature maps from the contracting path to ensure that the upsampled and cropped features align correctly. The final layer employs a single 1x1 convolution to convert the features into the desired number of class labels. The entire network consists of 23 convolutional layers. For the final segmentation map to be seamless, the input image size must be selected carefully, ensuring that all downsampling steps occur in layers with even width and height, thus preventing mismatches during upsampling in the expanding path [29].

5 Implementation of the algorithm

This section describes the development and implementation of an algorithm designed to detect glaucoma through the analysis of retinal fundus images. The proposed algorithm employs advanced image processing and machine learning techniques to analyze retinal fundus images, which are photographs of retinal fundus.

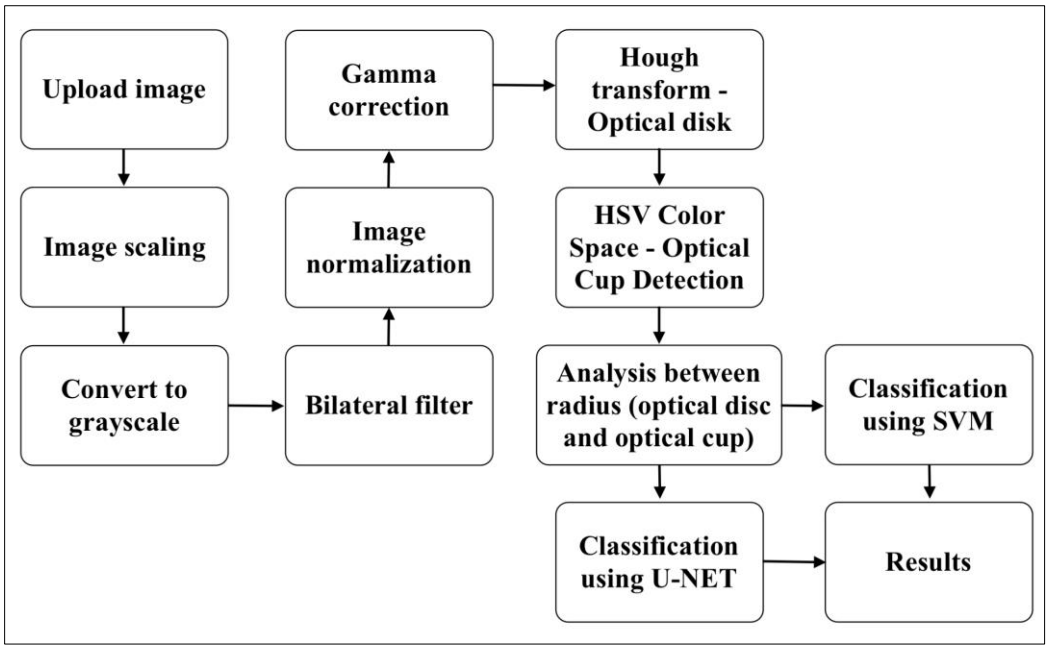

Figure 2 Flowchart showing the process and steps of the algorithm

Figure 2 shows the flow chart of the steps to follow of the implemented algorithm. The implementation of the algorithm was carried out in Python with its respective tools and libraries.

The steps shown in Figure 2 are explained below:

5.1.1 Upload image

From the OpenCv library in Python, the image to be read is chosen for subsequent processing and analysis, the image is saved in a variable that represents three $N \times M$ arrays (RGB). This image is a retinal fundus photograph obtained from the database ("The Brazil Glaucoma database"), labeled if the patient has glaucoma.

5.1.2 Image scaling

Due to the nature of the image, the need to always have the same dimensions or scaling, and the patterns that are sought within it, the image is resized to a size of 355x255 pixels.

5.1.3 Convert to grayscale

For a lower computational cost, it is necessary to reduce the complexity of the data, eliminating color information that is not necessary for glaucoma detection, and allowing us to focus on the structural characteristics of the retina. Therefore, obtaining gray scale is applied to the RGB image, since it is only a matrix now, it facilitates subsequent processing and the detection of features in the images.

5.1.4 Bilateral filter

Applying a bilateral smoothing filter aims to reduce noise while preserving the edges of the image. This filter helps to smooth homogeneous regions of the image, thereby reducing noise, and to preserve important details at the edges, preventing them from blurring as they might with other types of smoothing. It is used in this algorithm to preprocess the image to obtain better results from subsequent procedures.

5.1.5 Image normalization

Using the cv2.normalize function, image intensity levels are adjusted or normalized. It is important to standardize images before performing subsequent analyses, ensuring that lighting variations do not affect the processing results.

5.1.6 Gamma correction

A gamma correction with a gamma value of 2.5 is applied to the image to increase the contrast of the darker areas, thus highlighting the edges, this will help the segmentation processes. The result of the gamma correction is seen in Figure 3.

Figure 3 Gamma correction applied to the analysis image

5.2 Hough transform – optical disk detection

The Hough Circle Transform is a robust shape detection technique, is employed to identify circular structures within the image. Specifically, the outermost circle, corresponding to the optic disc, is localized. Isolation of the optic disc is a critical preprocessing step for glaucoma analysis. Upon detection, the coordinates of the optic disc are utilized to graphically overlay a circular marker onto the original image.

5.2.1 HSV Color Space – Optical Cup Detection

The HSV Color Space technique is used to locate the brightest circle in a fundus photograph of the retina, which represents the optical cup. This technique separates color information into components where "Value" means brightness. By analyzing the 'Value' component in HSV, the algorithm identifies the brightest regions of the image, which helps in accurate detection and segmentation.

5.2.2 Analysis between radius (optical desic and optical cup)

After isolating the optic disc, the radius of detected circles in the image are measured and analyzed. The process begins with image preparation and defining color ranges. Circle detection utilizes the Hough transform method on color masks generated for each color range. The largest circle in each case is detected, assuming it corresponds to the optic disc (in blue) and the optic nerve cup (in green).

Following this, the CDR is calculated based on the detected green and blue circles' radius. This standard measure assesses glaucoma risk; a higher CDR indicates a greater likelihood of glaucoma. Figure 4 shows the results of the radius measurement and the CDR calculation.

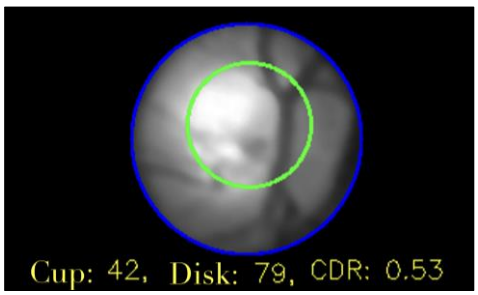

Figure 4 Detection of the radius of the cup and the optical disc

5.3 Classification using SVM

CDR, cup radius, disk radius, and the label are the input parameters for SVM, the labels categorizing images as "Normal" or "Glaucoma". SVM parameters, such as a linear kernel, are selected for this binary classification problem, alongside

adjustable regularization, kernel type, and loss function. Feature extraction begins with numeric labeling (0 for normal, 1 for glaucoma).

For SVM model training, features are scaled using StandardScaler to ensure uniformity. Data is split into training and test sets using train_test_split (80%-20%).

Model evaluation on the test set includes accuracy computation and a classification report showing precision, recall, f1-score, and support for each class. Predictions are visualized with random test set images and their predicted and actual labels using matplotlib.

5.4 Classification using U-NET

The process to create, train, and evaluate a classification model using U-Net begins with the input parameter: the image after the preprocessing stages of grayscale conversion, normalization and scaling. Subsequently, the U-Net architecture adapted for classification is defined, incorporating convolutional layers, max-pooling layers, dropout layers, and dense layers.

For training, categorical cross-entropy is used as the loss function to optimize classification. The Adam optimizer is employed with a learning rate of 1e-4. The batch size is set to 8, and the number of epochs is 10. During training, the dataset is split into training and testing subsets using the train_test_split function (80%-20%).

6 Results

This section presents the performance evaluation of the proposed SVM and U-NET classifiers for glaucoma detection using retinal fundus images. The dataset consisted of 316 images, equally divided into glaucomatous and non-glaucomatous groups. For both classifiers, an 80% training and 20% validation data split was employed.

6.1 Comparison

The SVM model outperforms the U-Net model in terms of precision, recall, F1-score, and overall accuracy for both "Normal" and "Glaucoma" classifications. While U-Net shows a slightly lower precision for both classes, it compensates with a high recall for "Glaucoma". The SVM model achieves a higher balance and overall accuracy, making it the more robust classifier in this comparison. The comparison of the results of both classifiers is shown in Table 2.

Table 2 Comparison of result metrics between SVM and U-NET

Metric	SVM	U-Net
Precision (Normal)	0.94	0.93
Recall (Normal)	0.97	0.81
F1-Score (Normal)	0.95	0.87
Precision (Glaucoma)	0.97	0.83
Recall (Glaucoma)	0.94	0.94
F1-Score (Glaucoma)	0.95	0.88
Accuracy	95%	88%

7 Conclusion

The comparative analysis of the SVM and U-Net models reveals notable differences in performance metrics for the classification of optical disc images. The SVM model demonstrates superior overall efficacy, achieving higher precision, recall, F1-scores, and accuracy across both "Normal" and "Glaucoma" classifications. Specifically, the SVM model exhibits a precision of 0.94 for "Normal" and 0.97 for "Glaucoma," with corresponding recall values of 0.97 and 0.94, respectively. Its overall accuracy of 95% underscores its robustness and reliability in image classification tasks.

In contrast, the U-Net model, while showing strong performance, lags behind SVM in several key metrics. Precision for "Normal" and "Glaucoma" is lower at 0.93 and 0.83, respectively, with recall values of 0.81 for "Normal" and 0.94 for "Glaucoma." The F1-scores of 0.87 for "Normal" and 0.88 for "Glaucoma" further reflect a lesser balance between

precision and recall compared to the SVM model. The U-Net model achieves an overall accuracy of 88%, which, although significant, is slightly inferior to that of the SVM model.

These results highlight the SVM model's superior classification performance and stability, making it the preferred choice for applications requiring high precision and accuracy. However, the U-Net model's higher recall for "Glaucoma" suggests its potential utility in scenarios where the detection of this condition is of paramount importance, despite its lower overall accuracy. Future work may explore further optimization of the U-Net architecture to enhance its precision and balance, potentially bridging the performance gap observed in this study.

Compliance with ethical standards

Disclosure of conflict of interest

No conflict of interest to be disclosed.

References

[1] M. H. Sarhan, M. A. Nasseri, D. Zapp, M. Maier, and C. P. Lohmann, “Machine learning techniques for ophthalmic data processing: A review,” pp. 1–14, 2020, doi: 10.1109/JBHI.2020.3012134.

[2] A. Shabbir et al., “Detection of glaucoma using retinal fundus images: A comprehensive review,” Mathematical Biosciences and Engineering, vol. 18, no. 3, pp. 2033–2076, 2021, doi: 10.3934/MBE.2021106.

[3] A. Sinha, A. R. P, and N. N. S, “Eye tumour detection using deep learning,” in Proc. 2021 IEEE 7th Int. Conf. Bio Signals, Images and Instrumentation, ICBSII 2021, 2021, doi: 10.1109/ICBSII51839.2021.9445172.

[4] R. Sarki, K. Ahmed, and Y. Zhang, “Early detection of diabetic eye disease through deep learning using fundus images,” EAI Endorsed Trans. Pervasive Health Technol., vol. 6, no. 22, pp. 1–8, 2020, doi: 10.4108/eai.13-7-2018.164588

[5] N. Navaitthiporn, P. Rithcharung, C. Wongpa, T. Treebupachatsakul, and S. Pechprasarn, “Auto focusing ophthalmoscope for smartphone,” in Proc. 2020 8th E-Health and Bioengineering Conf., EHB 2020, pp. 20–23, 2020, doi: 10.1109/EHB50910.2020.9280158.

[6] C. Braganca, J. M. Torres, C. Pinto, and L. Oliveira, “Detection of glaucoma on fundus images using deep learning on a new image set obtained with a smartphone and handheld ophthalmoscope enhanced reader,” Healthcare, vol. 10, no. 2345, 2022.

[7] R. Robles et al., “A systematic review of digital ophthalmoscopes in medicine,” Clin. Ophthalmol., vol. 17, no. Sep., pp. 2957–2965, 2023, doi: 10.2147/OPTH.S423845.

[8] J. Carrillo, L. Bautista, J. Villamizar, J. Rueda, M. Sanchez, and D. Rueda, “Glaucoma detection using fundus images of the eye,” in Proc. 2019 22nd Symp. Image, Signal Processing and Artificial Vision, STSIVA 2019 - Conf. Proc., Apr. 2019, doi: 10.1109/STSIVA.2019.8730250.

[9] K. A. Thakoor, S. Member, S. C. Koorathota, S. Member, and C. Donald, “Robust and interpretable convolutional neural networks to detect glaucoma in optical coherence tomography images,” IEEE Trans. Biomed. Eng., pp. 1–11, 2020, doi: 10.1109/TBME.2020.3043215.

[10] R. Shinde, “Intelligence-based medicine glaucoma detection in retinal fundus images using U-Net and supervised machine learning algorithms,” Intell. Based Med., vol. 5, p. 100038, 2021, doi: 10.1016/j.ibmed.2021.100038.

[11] A. N. A., A. S. S., A. S., L. P., and D. C. D., “Glaucoma detection using fundus images of the retina,” Appl. Comput. Eng., vol. 2, no. 1, pp. 283–290, 2023, doi: 10.54254/2755-2721/2/20220641.

[12] M. S. Puchaicela-Lozano et al., “Deep learning for glaucoma detection: R-CNN ResNet-50 and image segmentation,” J. Adv. Inf. Technol., vol. 14, no. 6, pp. 1186–1197, 2023, doi: 10.12720/jait.14.6.1186-1197.

[13] R. Verma, L. Shrinivasan, and B. Hiremath, “Machine learning classifiers for detection of glaucoma,” IAES Int. J. Artif. Intell., vol. 12, no. 2, pp. 806–814, 2023, doi: 10.11591/ijai.v12.i2.pp806-814.

[14] C. S. Fathima and E. N. Subhija, “Glaucoma detection using fundus images and OCT images,” in Proc. Int. Conf. Syst. Energy and Environ., pp. 1–7, 2019.

[15] Y. George, B. J. Antony, H. Ishikawa, G. Wollstein, and J. S. Schuman, “Attention-guided 3D-CNN framework for glaucoma detection and structural-functional association using volumetric images,” IEEE J. Biomed. Health Inform., pp. 1–10, 2020, doi: 10.1109/JBHI.2020.3001019.

[16] E. O. Rodrigues, A. Conci, P. Liatsis, and S. Member, “ELEMENT: Multi-modal retinal vessel segmentation based on a coupled region growing and machine learning approach,” IEEE J. Biomed. Health Inform., vol. 24, no. 12, pp. 3507–3519, 2020.

[17] F. Abdullah, R. Imtiaz, H. A. Madni, H. A. Khan, and T. M. Khan, “A review on glaucoma disease detection using computerized techniques,” pp. 37311–37333, 2021.

[18] M. Hasan, “Source and camera independent ophthalmic disease recognition from fundus image using neural network,” pp. 28–30, 2019.

[19] R. Amin, A. Ahmed, S. Shabih Ul Hasan, and H. Akbar, “Multiple eye disease detection using deep learning,” Found. Univ. J. Eng. Appl. Sci., vol. 3, no. 2, pp. 14–26, 2023, doi: 10.33897/fujeas.v3i2.689.

[20] R. Sarki, K. Ahmed, H. U. A. Wang, and Y. Zhang, “Automatic detection of diabetic eye disease through deep learning using fundus images: A survey,” IEEE Access, 2020, doi: 10.1109/ACCESS.2020.3015258.

[21] O. Bernabé, E. Acevedo, A. Acevedo, R. Carreño, and S. Gómez, “Classification of eye diseases in fundus images,” IEEE Access, 2021, doi: 10.1109/ACCESS.2021.3094649.

[22] C. Bragança, J. M. Torres, C. Pinto, and L. Oliveira, "Detection of Glaucoma on Fundus Images Using Deep Learning on a New Image Set Obtained with a Smartphone and Handheld Ophthalmoscope Enhanced Reader.pdf," Healtcare, vol. 10, no. 2345, 2022.

[23] A. Grzybowski (Ed.), Artificial Intelligence in Ophthalmology. 1st ed. Switzerland: Springer Nature Switzerland AG,2021. doi: 10.1007/978-3-030-78601-4.

[24] L. Caraffa, J. -P. Tarel and P. Charbonnier, "The Guided Bilateral Filter: When the Joint/Cross Bilateral Filter Becomes Robust," in IEEE Transactions on Image Processing, vol. 24, no. 4, pp. 1199-1208, April 2015, doi: 10.1109/TIP.2015.2389617.

[25] L. Huang, G. Cao and L. Yu, "Efficient contrast enhancement with truncated adaptive gamma correction," 2016 9th International Congress on Image and Signal Processing, BioMedical Engineering and Informatics (CISP-BMEI), Datong, China, 2016, pp. 189-194, doi: 10.1109/CISP-BMEI.2016.7852706.

[26] S. Kulandaivel and R. K. Jeyachitra, "Combined image Hough transform based simultaneous multi-parameter optical performance monitoring for intelligent optical networks," Opt. Fiber Technol., vol. 79, no. 103357, 2023. doi: 10.1016/j.yofte.2023.103357.

[27] F. Sabry, Color Space: Exploring the Spectrum of Computer Vision. One Billion Knowledgeable, Computer Vision Series, 2024.

[28] M. Zakariah, M. Al-Razgan, and T. Alfakih, "Pathological voice classification using MEEL features and SVM-TabNet model," Speech Commun., vol. 162, no. 103100, 2024. doi: 10.1016/j.specom.2024.103100.

[29] O. Ronneberger, P. Fischer, and T. Brox, "U-Net: Convolutional Networks for Biomedical Image Segmentation," in Medical Image Computing and Computer-Assisted Intervention – MICCAI 2015, Springer International Publishing, 2015, pp. 234–241.